Analysis of Analog and Digital MRC in Massive MU-MIMO Systems over Correlated Channels

Shuang Li, Peter J. Smith, Pawel A. Dmochowski, and Jingwei Yin

***Abstract*—While digital multi-user (MU) maximal ratio combining (MRC) is well understood, relatively few analytical results exist for analog MU-MRC. For example, it has recently been shown that MU system performance is highly dependent on the correlation model used, but the scope is limited to digital processing. Thus, in this paper we compare the performance of analog and digital MRC, focusing on the effects of correlation. We begin by deriving the expected signal and interference powers, demonstrating that the signal-to-interference ratio decreases with correlation when users have the same correlation matrices, while it increases when their correlation matrices are different. These finite system results are then extended by deriving asymptotic signal-to-interference-and-noise ratio expressions for both analog and digital MRC for the benchmark scenarios of uncorrelated and perfectly correlated Rayleigh channels. Here, we once again demonstrate that the performance is critically dependent on the correlation scenario.**

***Index Terms*—Analog MRC, correlation, digital MRC, MU-MIMO.**

I. INTRODUCTION

MASSIVE multiple user multiple input multiple output (MU-MIMO) is a key technique for future broadband networks as it provides many benefits. Large-scale antenna systems can increase system capacity and improve energy efficiency on the order of 10 times or more simultaneously [1]. They not only reduce transmit power but also average out small-scale fading as random matrices start to look deterministic, which also offers benefits in robustness and reliability [1]. However, when the system is able to serve more users due to the number of antennas increasing at the base station (BS), the resulting interference among users can have a negative impact on the overall system performance. Zero-forcing (ZF) can suppress the inter-user interference at the cost of more computational complexity. For example, the matrix inverse required by ZF has a complexity order of $O(K^3)$ where K is the number of user data streams. Thus, taking communication overheads and complexity into consideration, simplified processing is required.

Among linear processing techniques, digital maximal ratio combining (MRC) and analog MRC[1], due to their simplicity and efficiency, are more practical in massive MU-MIMO systems. The two methods passively reduce interference by taking advantage of favourable propagation[2]. An additional benefit of MRC is its suitability to distributed systems - the processing can be performed independently at each antenna cluster, without additional information exchange [2]. Analog MRC, by utilizing only one radio frequency chain, further reduces hardware cost and power consumption compared with digital MRC. Due to the presence of only a single RF-chain, the average spectral efficiency of massive MIMO systems with pure analog processing is less than the digital counterpart due to the inability to weight the amplitude of the incoming signal. However, despite this disadvantage, most of the current commercial 5G-NR street-macro and micro-cellular solutions within the FR2 bands are based on analog processing [3]. Hence, it is important to analyze analog processing. We note that most analytical work concerning analog MRC is from the perspective of modulation, outage probability and bit error probability [4]–[11].

Since there are more antennas which are closely-spaced in one physical location, massive MIMO suffers more from spatial correlation than conventional MIMO systems [12]. Although some research shows that system performance is critically dependent on the type of correlation model, they demonstrate this using simulations rather than mathematical analysis.

Although the asymptotic behaviour of large systems with correlation (equal for all users) has been well studied (see [2], [13], [14]), the effect on performance is not straightforward. Some studies demonstrate a negative impact [15], [16] and others suggest a positive impact [17], [18]. The above studies assume equal correlation among users. Recently, the impact of correlation on system performance has been shown to be

Manuscript received March 4, 2021; revised August 13, 2021; approved for publication by Sooyong Choi, Division II Editor September 14, 2021.

The work of S. Li was supported by the Fundamental Research Funds for the Central Universities (XK2050021008).

The work of J. Yin was supported by the National Natural Science Foundation of China (61901136).

S. Li is with Qingdao Innovation and Development Center of Harbin Engineering University and also with the College of Underwater Acoustic Engineering, Harbin Engineering University, Harbin 150001, P.R.China, email: shuangli@hrbeu.edu.cn.

P. J. Smith is with the School of Mathematics and Statistics, Victoria University of Wellington, PO Box 600 Wellington 6140, New Zealand, email: peter.smith@ecs.vuw.ac.nz.

P. A. Dmochowski is with the School of Engineering and Computer Science, Victoria University of Wellington, PO Box 600 Wellington 6140, New Zealand, email: pawel.dmochowski@ecs.vuw.ac.nz.

J. Yin is with the College of Underwater Acoustic Engineering, Harbin Engineering University, Harbin 150001, P.R.China, email: yinjingwei@hrbeu.edu.cn.

Digital Object Identifier: 10.23919/JCN.2021.000033

[1] Analog MRC is also known as equal gain combining (EGC) in classical literature. We chose the term analog MRC in order to align the work with hybrid processing literature.

[2] Favourable propagation refers to the scenario where the number of BS antennas becomes large, causing the user channels to become orthogonal automatically. This enables simple, linear processing techniques, such as MRC, to maximize the system capacity.

1229-2370/21/$10.00 © 2021 KICS

highly dependent on the correlation model [19], [20]. Furthermore, results and measurements in [20] demonstrate that correlation variability among users enhances the performance of digital MRC. It is intuitively clear that equal correlation structures across users hinders performance as similar statistics implies more similar channels and increased interference. However, this understanding is relatively recent. Many papers still model a multi-user system with equal correlation matrices per user (see the example references [21]–[24]). It is also well known that the level of correlation can impact on system performance both positively and negatively, depending on the processing. However, the joint effect of correlation level and variability across users is little studied. Hence, we were motivated to further explore the impact of both correlation variability and the joint effects of correlation variability and level.

Hence, in this paper we provide new insights into the impact of correlation (including its heterogeneity) on the SINR and spectral efficiency (SE) behaviour of digital MRC and the first such results for analog MRC. Specifically,

- We derive closed form expressions for the expected signal and interference power, and use these to show that the signal-to-interference ratio (SIR) behaviour is highly dependent on the correlation heterogeneity across users.
- We derive a closed-form SIR expression based on the exponential correlation model. The 3D surface plots based on this expression give great insight into the circumstances where high correlation can improve system performance. We also show similar behaviour under the one-ring correlation model.
- We derive new asymptotic results for analog and digital MRC SINR in Rayleigh fading for the benchmark scenarios of uncorrelated and perfectly correlated channels, when both the number of users and antennas go to infinity. For the latter, the system performance suggests that digital and analog MRC would have the same asymptotic behaviour. For general correlated channels, the limits are shown to be critically dependent on the correlation heterogeneity, specifically, correlation is detrimental with equal correlation, but beneficial with variation across users. Depending on the assumptions, the resulting SINR can either vanish in the limit or converge to a constant. For uncorrelated channels, from the derived expression of SINR for i.i.d. Rayleigh fading, around 21.5% performance loss occurs with analog MRC compared with digital MRC.

II. SYSTEM MODEL

We consider an uplink massive MIMO system with N antennas serving K single antenna users. The $N \times 1$ channel vector for user i can be written as $\mathbf{h}_i = \mathbf{R}_i^{1/2}\mathbf{u}_i$, where $\mathbf{u}_i \sim \mathcal{CN}(\mathbf{0}, \mathbf{I})$, $\mathbf{R}_i = \beta_i \mathbf{\Sigma}_i$, $\mathbf{\Sigma_i}$ is the $N \times N$ spatial correlation matrix and β_i is the large-scale link gain. As we are analysing convergence issues under three scenarios, we are not modeling the link gain based on classic path-loss and log-normal shadowing because the substantial variation caused by shadowing will make it inconvenient to see the limiting effects. We adopt a similar approach to that in [14] to counter this problem. We have two models for β_i, equal and unequal power for each user. We use the equal link gain case as a reference and we assume $\beta = 1$ for all users. For the unequal case, we set $\beta_1 = 1$ for the desired user and for the interfering users, we select β_l from the exponential decay function $Ae^{-\lambda x}$ such that the average interference power is equal to β_1. As there is no zero link gain in practice, we guarantee a minimum link gain by cutting off the least 10% values of $Ae^{-\lambda x}$, which means β_l has a range of $[(1/10)A, A]$. Hence, β_l is given by $\beta_l = Ae^{-(l-2)\lambda}$. This model gives $K-1$ values of β_l decaying exponentially over $[(1/10)A, A]$. The channel matrix is $\mathbf{H} = [\mathbf{h}_1\mathbf{h}_2 \cdots \mathbf{h}_K]$. We assume perfect channel knowledge at the BS and equal transmit power, P_t, for each user. Thus, the received signal at the BS can be expressed as

$$\mathbf{y} = \sqrt{P_\text{t}}\mathbf{H}\mathbf{s} + \mathbf{n}, \tag{1}$$

where $\mathbf{n} \sim \mathcal{CN}(\mathbf{0}, {\sigma_\text{n}}^2\mathbf{I})$ is white Gaussian noise, $\mathbf{s}$ is the data symbol vector from the K users and $\mathbb{E}[\mathbf{s}\mathbf{s}^H] = \mathbf{I}$. Without loss of generality, σ_n^2 is assumed to be 1. The signal after combining at the BS to detect the ith user is given by

$$\tilde{\mathbf{y}}_i = \sqrt{P_\text{t}}\mathbf{g}_i^\text{H}\mathbf{h}_i s_i + \sqrt{P_\text{t}}\sum_{l=1,l\neq i}^{K}\mathbf{g}_i^\text{H}\mathbf{h}_l s_l + \mathbf{g}_i^\text{H}\mathbf{n}, \tag{2}$$

where $\mathbf{g}_i = \mathbf{h}_i$ for digital MRC and $\mathbf{g}_i = \hat{\mathbf{h}}_i$ for analog MRC, where $\hat{\mathbf{h}}_i = \exp(j\angle\mathbf{h}_i)$ and $\angle\mathbf{h}_i$ indicates the vector of angles of $\mathbf{h}_i$. The corresponding SINR is given by [25]

$$\text{SINR}_i = \frac{P_\text{t}|\mathbf{g}_i^\text{H}\mathbf{h}_i|^2}{P_\text{t}\sum_{l=1,l\neq i}^{K}|\mathbf{g}_i^\text{H}\mathbf{h}_l|^2 + \mathbf{g}_i^\text{H}\mathbf{g}_i}. \tag{3}$$

To enable the analysis, we apply the following commonly used approximation: if $X = \sum X_i$ and $Y = \sum Y_i$ are both sums of non-negative random variables, then $\mathbb{E}\left[\log_2(1 + X/Y)\right] \approx \log_2(1 + \mathbb{E}[X]/E[Y])$ [26]. Independence between X and Y is not required and the result becomes more accurate when the number of the summation terms in X and Y is large [26]. This behaviour is due to the law of large numbers [26] where the numerator and denominator approach their mean values and their variances become small. On the uplink, using (3), this approximation gives the per-user spectral efficiency of

$$\mathbb{E}[\text{R}] \approx \log_2\left\{1 + \frac{P_\text{t}\mathbb{E}|\mathbf{g}_i^\text{H}\mathbf{h}_i|^2}{P_\text{t}\mathbb{E}\left[\sum_{l=1,l\neq i}^{K}|\mathbf{g}_i^\text{H}\mathbf{h}_l|^2 + \mathbf{g}_i^\text{H}\mathbf{g}_i\right]}\right\}. \tag{4}$$

The expression in (4) allows for the analysis of achievable rates for linear processing schemes, such as matched filter (MF) ZF, minimum mean squared error (MMSE) and to gain new insights into their performance, in particular the effects of correlation.

The expectation of the signal and interference terms in (4) for digital MRC are, respectively, given by [27]

$$\mathbb{E}\left[P_\text{t}|\mathbf{g}_i^\text{H}\mathbf{h}_i|^2\right] = P_\text{t}\beta_i^2[\text{tr}(\mathbf{\Sigma}_i^2) + N^2], \tag{5}$$

$$\mathbb{E}\left[P_{\rm t}\sum_{l\neq i}|\mathbf{g}_i^{\rm H}\mathbf{h}_l|^2\right] = P_{\rm t}\beta_i\sum_{l\neq i}\beta_l{\rm tr}(\mathbf{\Sigma}_i\mathbf{\Sigma}_l). \tag{6}$$

The relationship between correlation and performance is seen in (5) and (6) via the terms $\text{tr}(\mathbf{\Sigma}_i^2)$ and $\text{tr}(\mathbf{\Sigma}_i\mathbf{\Sigma}_l)$. To explore this relationship, consider the exponential correlation model in [28] where $(\mathbf{\Sigma}_i)_{rs} = \rho^{|s-r|}\text{exp}(j(s-r)\phi_i)$, so that users have the same amplitude correlation parameter, ρ, but user specific phases, $\phi_i \sim U[0, 2\pi]$. Using this model, straightforward algebra allows $\text{tr}(\mathbf{\Sigma}_i\mathbf{\Sigma}_l)$ to be written as (7), where $\Delta = \phi_i - \phi_j$. Obviously, $\text{tr}(\mathbf{\Sigma}_i\mathbf{\Sigma}_l)$ is a function of ρ and Δ. Less obviously, the relationship between interference and ρ is different for different values of Δ. To see this, consider the two special cases of (7):

$$\text{tr}(\mathbf{\Sigma}_i\mathbf{\Sigma}_l) = \frac{N(1-\rho^2)(1+\rho^2)+2\rho^{2N+2}-2\rho^2}{(1-\rho^2)^2},\ \Delta=0, \tag{8}$$

$$\text{tr}(\mathbf{\Sigma}_i\mathbf{\Sigma}_l) = \frac{N(1-\rho^8)+4\rho^4-4(-1)^{N/2}\rho^{2N+4}}{(1+\rho^4)^2},\ \Delta=\frac{\pi}{2}, \tag{9}$$

where (9) is for the case of even N. When the phase parameters are aligned ($\Delta = 0$), the correlation matrices are identical, the first numerator term of (8) dominates and the interference increases with ρ. When the two phases are orthogonal ($\Delta = \pi/2$), the first numerator term in (9) dominates and the interference decreases with ρ. Hence, increasing the size of the correlation can have opposite effects when users experience the same correlation matrix ($\phi_i = \phi_j$) and when the correlation matrices differ ($\phi_i - \phi_j = \pi/2$). Equivalent results to (5) and (6) for analog MRC are available in [25] but are given in terms of Gaussian hypergeometric functions which make interpretation difficult. Hence, we look at the extreme cases of zero and perfect correlation in Section III.

III. ASYMPTOTIC SINR ANALYSIS

We derive the asymptotic SINR for analog and digital MRC under the two benchmark scenarios of i.i.d. and perfectly correlated Rayleigh fading. We assume N and K grow at the same rate, so that $\alpha = N/K$ is fixed and this asymptotic regime is described by $\lim_{N\to\infty}$. The derivations require the strong law of large numbers (S.L.L.N), the version given in [29, Th. 5.4.3] (**Result 1**) being adequate for these proofs.

Result 1: If $X_1, X_2, \cdots$ are independent with finite means $\mu_1, \mu_2, \cdots$ and variances $\sigma_1^2, \sigma_2^2, \cdots$, then $(1/L)\sum_{n=1}^{L} X_n \xrightarrow{\text{a.s.}} \mu$, a.s. $L \to \infty$, where $\mu = \lim_{L\to\infty}\left((1/L)\sum_{n=1}^{L}\mu_n\right)$ if $\sum_{n=1}^{L}(1/L^2)\text{Var}(X_n) < \infty$ [29, Th. 5.4.3].

A. Asymptotic Analysis for i.i.d. Rayleigh Fading

First, for digital MRC, from (3), the interference power is,

$$\begin{aligned} P_{\rm t}\sum_{l\neq i}^{K}|\mathbf{h}_i^{\rm H}\mathbf{h}_l|^2 &= P_{\rm t}\sum_{l\neq i}^{K}\mathbf{h}_l^{\rm H}\mathbf{h}_i\mathbf{h}_i^{\rm H}\mathbf{h}_l \\ &= \sum_{l=1,l\neq i}^{K}\beta_i\beta_l\mathbf{u}_l^{\rm H}\text{diag}\{\mathbf{u}_i^{\rm H}\mathbf{u}_i, 0, 0, \cdots\}\mathbf{u}_l \\ &= \sum_{l=1,l\neq i}^{K}\beta_i\beta_l|u_{l1}|^2|\mathbf{u}_i\mathbf{u}_i^{\rm H}|. \end{aligned} \tag{10}$$

In (10), u_{l1} is the first element of $\mathbf{u}_l$ and the second equality follows from the rank-1 eigen-decomposition of $\mathbf{h}_i\mathbf{h}_i^{\rm H}$. The desired signal power is $P_{\rm t}\left(\mathbf{h}_i^{\rm H}\mathbf{h}_i\right)^2 = P_{\rm t}\beta_i^2(\mathbf{u}_i^{\rm H}\mathbf{u}_i)^2$ and the noise power is $\mathbf{h}_i^{\rm H}\mathbf{h}_i = \beta_i\mathbf{u}_i^{\rm H}\mathbf{u}_i$. Substituting into (3) and simplifying gives

$$\text{SINR}_i^{\rm D} = \frac{P_{\rm t}\beta_i\mathbf{u}_i^{\rm H}\mathbf{u}_i/N}{\frac{P_{\rm t}(K-1)}{N}\sum_{l\neq i}^{K}\frac{\beta_l|u_{l1}|^2}{K-1} + \frac{1}{N}}, \tag{11}$$

where D denotes digital MRC. Using the S.L.L.N (**Result 1**), the numerator of (11) converges almost surely (a.s.), giving

$$\lim_{N\to\infty}\beta_i\frac{\left(|\mathbf{u}_i\mathbf{u}_i^{\rm H}|\right)}{N} = \lim_{N\to\infty}\frac{\beta_i}{N}\sum_{r=1}^{\rm N}|u_{ir}|^2 \xrightarrow{\text{a.s.}} \beta_i\mathbb{E}(|u_{i1}|^2) = \beta_i. \tag{12}$$

Similarly, the denominator of (11) converges almost surely,

$$\lim_{K-1\to\infty}\left(\frac{\sum_{l=1, l\neq i}^{K}\beta_l(u_{l1})^2}{K-1}\right) \xrightarrow{\text{a.s.}} \bar{\beta}.$$

Thus, finally we get

$$\lim_{N,K\to\infty}\text{SINR}_i^{D} = \frac{\beta_i}{\bar{\beta}}\alpha, \tag{13}$$

where $\bar{\beta} = \lim_{N\to\infty}\sum_{i=1}^{K}\beta_i/K$ is the asymptotic mean of the link gains. For the equal β case, (13) can be written as

$$\lim_{N,K\to\infty}\text{SINR}_i^{D} = \alpha. \tag{14}$$

For analog MRC, similar steps lead to the result

$$\text{SINR}_i^{\rm A} = \frac{P_{\rm t}\beta_i|\hat{\mathbf{u}}_i^{\rm H}\mathbf{u}_i/N|^2}{\frac{P_{\rm t}(K-1)}{K-1}\sum_{l\neq i}^{K}\beta_l\left|\frac{\hat{\mathbf{u}}_i^{\rm H}\mathbf{u}_l}{N}\right|^2 + \frac{1}{N}}, \tag{15}$$

using $\hat{\mathbf{h}}_i = \sqrt{\beta_i}\hat{\mathbf{u}}_i$. For the numerator, the S.L.L.N gives

$$\frac{\hat{\mathbf{u}}_i^{\rm H}\mathbf{u}_i}{N} = \sum_{r=1}^{N}\frac{|u_{ir}|}{N} \xrightarrow{\text{a.s.}} \mathbb{E}(|u_{ir}|) = \Gamma\left(\frac{3}{2}\right) = \frac{\sqrt{\pi}}{2}. \tag{16}$$

For the interference term, we note that

$$\sum_{l=1,l\neq i}^{K}\beta_l|\hat{\mathbf{u}}_i^{\rm H}\mathbf{u}_l|^2 = \sum_{\substack{l=1\\ l\neq i}}^{K}\beta_l\mathbf{u}_l^{\rm H}\text{diag}\{N, 0, 0, \cdots\}\mathbf{u}_l \tag{17}$$

$$= \sum_{l=1,l\neq i}^{K}\beta_l|u_{l1}|^2 N, \tag{18}$$

$$\frac{2\rho^{2N+2}\left(\cos((N+1)\Delta)-2\rho^2\cos(N\Delta)+\rho^4\cos((N-1)\Delta)\right)+N(1-\rho^8)+4\rho^4+\cos(\Delta)\left((2N-2)\rho^6-(2N+2)\rho^2\right)}{(1-2\rho^2\cos(\Delta)+\rho^4)^2}. \tag{7}$$

which follows from the rank-1 eigen-decomposition of $\hat{\mathbf{u}}_i\hat{\mathbf{u}}_i^{\mathrm{H}}$. Thus, from the S.L.L.N, the interference term in (15) is

$$P_{\mathrm{t}}\frac{K-1}{N}\sum_{l=1,l\neq i}^{K}\beta_l\frac{|u_{l1}|^2}{(K-1)}\xrightarrow{\text{a.s.}}P_{\mathrm{t}}\frac{\bar{\beta}}{\alpha}. \tag{19}$$

Substituting (16) and (19) into (15), we obtain

$$\lim_{N\to\infty}\mathrm{SINR}_i^{\mathrm{A}}=\frac{\pi\beta_i}{4\bar{\beta}}\alpha. \tag{20}$$

Compared with digital MRC, analog MRC suffers a $(1-\pi/4)\times 100\approx 21.5\%$ performance loss in the asymptotic SINR.

B. Asymptotic Analysis, Perfect Correlation, Equal Matrices

Consider the perfectly correlated channel where $\mathbf{R}_i=\beta_i\mathbf{\Sigma}_i$ and all the elements of $\mathbf{\Sigma}_i$ equal one. Here, $\mathbf{h}_i=\mathrm{h}_{i1}[11\cdots 1]^T$ and $\hat{\mathbf{h}}_i=\exp(j\angle\mathrm{h}_{i1})[11\cdots 1]^T$. Substituting the perfectly correlated channels and associated combiners into (3) gives:

$$\begin{aligned}\mathrm{SINR}_i^D&=\frac{P_t(|h_{i1}|^2|N|)^2}{P_t\sum_{\substack{l=1\\l\neq i}}^K[|h_{i1}^*h_{l1}N|]^2+|h_{i1}|^2N}\\&=\frac{P_t|h_{i1}|^4N^2}{P_t\sum_{\substack{l=1\\l\neq i}}^K[|h_{i1}|^2|h_{l1}|^2N^2]+|h_{i1}|^2N}\\&=\frac{\beta_i|u_{i1}|^2}{\sum_{\substack{l=1\\l\neq i}}^K\beta_l|u_{l1}|^2+\frac{1}{P_tN}},\end{aligned} \tag{21}$$

and

$$\begin{aligned}\mathrm{SINR}_i^A&=\frac{P_t|h_{i1}|^2N^2}{P_t\sum_{\substack{l=1\\l\neq i}}^K\left[\left|\frac{h_{i1}^*}{|h_{i1}|}h_{l1}N\right|\right]^2+N}\\&=\frac{\beta_i|u_{i1}|^2}{\sum_{\substack{l=1\\l\neq i}}^K\beta_l|u_{l1}|^2+\frac{1}{P_tN}}.\end{aligned} \tag{22}$$

Thus, $\mathrm{SINR}_i^{\mathrm{A}}=\mathrm{SINR}_i^{\mathrm{D}}$ and dividing numerator and denominator by K, the S.L.L.N gives

$$\mathrm{SINR}_i^{\mathrm{A}}=\mathrm{SINR}_i^{\mathrm{D}}\xrightarrow{\text{a.s.}}0. \tag{23}$$

The SINRs vanish here due to the interference growth which occurs when all the user channels are aligned.

C. Asymptotic Analysis, Perfect Correlation, Unequal Matrices

Here we investigate two types of correlation structures for uniform linear arrays. The exponential correlation model in [28] has a user specific phase, $\phi_i\sim U[0,2\pi]$, for the correlation parameter and for perfect correlation (amplitude 1). The correlation matrix is defined by $(\mathbf{\Sigma}_i)_{rs}=\exp(j(s-r)\phi_i)$. The second model is the classic one-ring model [30], defined by,

$$(\mathbf{\Sigma}_i)_{rs}=\frac{1}{\mathrm{AS}}\int_{\theta_i-\mathrm{AS}/2}^{\theta_i+\mathrm{AS}/2}e^{-j2\pi d(r-s)\sin(\theta_i)d\theta_i}, \tag{24}$$

where AS is the angle spread, θ_i is the central angle for user i and d is the antenna spacing. For this model, taking the limit as the angle spread vanishes gives a perfectly correlated correlation matrix also defined by $(\mathbf{\Sigma}_i)_{rs}=\exp(j(s-r)\phi_i)$ but here, $\phi_i=2\pi d\sin(\theta_i)$. For both models, defining $\mathbf{a}_i=[1\ \exp(-j\phi_i)\ \exp(-j2\phi_i)\ \cdots\ \exp(-j(N-1)\phi_i)]^T$ allows the channel vectors to be written as $\mathbf{h}_i=\mathrm{h}_{i1}\mathbf{a}_i$. Following the steps in Section III-B the corresponding SINRs are

$$\mathrm{SINR}_i^{\mathrm{A}}=\mathrm{SINR}_i^{\mathrm{D}}=\frac{|h_{i1}|^2}{\sum_{l\neq i}^K|h_{l1}|^2\left|\frac{\mathbf{a}_i^H\mathbf{a}_l}{N}\right|^2+\frac{1}{P_{\mathrm{t}}N}}. \tag{25}$$

From (25), we see that the SINR depends on the limiting behaviour of the interference component denoted by I. We explore this limiting behaviour by deriving $\mathbb{E}(I)$:

$$\begin{aligned}\mathbb{E}(I)=&\frac{K-1}{N}\mathbb{E}(|h_{l1}|^2)\frac{1}{N}\mathbb{E}[|\mathbf{a}_i^H\mathbf{a}_l|^2]\\&\to\mu_I^\infty=\frac{1}{\alpha}\lim_{N\to\infty}\frac{1}{N}\mathbb{E}[|\mathbf{a}_i^H\mathbf{a}_l|^2]\end{aligned} \tag{26}$$

which can be written as

$$\begin{aligned}\mathbb{E}(I)&=\frac{1}{\alpha}\lim_{N\to\infty}\frac{1}{N}\sum_{h=0}^{N-1}\sum_{k=0}^{N-1}\mathbb{E}\left[e^{j(h-k)\phi_i}\right]\mathbb{E}\left[e^{-j(h-k)\phi_l}\right]\\&=\frac{1}{\alpha}\lim_{N\to\infty}\left\{1+2\sum_{r=1}^{N-1}(1-\frac{r}{N})|\mathbb{E}[e^{jr\phi_i}]|^2\right\}.\end{aligned} \tag{27}$$

Next, we derive $|\mathbb{E}[e^{jr\phi_i}]|$ for the two correlation models.

1) Exponential Correlation: The model in [28] has $\phi_i\sim U[0,2\pi]$ for which $\mathbb{E}[e^{jr\phi_i}]=0$ and $\mathbb{E}(I)\to 1/\alpha$. For the more general case where $\phi_i\sim U[a,b]$,

$$\begin{aligned}|\mathbb{E}[e^{jr\phi_i}]|=&\left|(b-a)^{-1}\int_a^b e^{jr\phi_i}d\phi_i\right|=\frac{2|\sin[0.5r(b-a)]|}{r(b-a)}\\&\leq 2/(r(b-a)).\end{aligned} \tag{28}$$

Substituting (28) into (27) we have,

$$\begin{aligned}\mathbb{E}(I)=&\frac{1}{\alpha}\left\{1+2\lim_{N\to\infty}\sum_{r=1}^{N-1}(1-\frac{r}{N})|\mathbb{E}[e^{jr\phi_i}]|^2\right\}\\&\leq\frac{1}{\alpha}\left\{1+\frac{8}{(b-a)^2}\lim_{N\to\infty}\left\{\sum_{r=1}^{N-1}\frac{1}{r^2}-\frac{1}{N}\sum_{r=1}^{N-1}\frac{1}{r}\right\}\right\},\end{aligned} \tag{29}$$

where $\sum_{r=1}^{N-1} 1/r^2 = \pi^2/6$, and

$$\frac{1}{N}\sum_{r=1}^{N-1}\frac{1}{r} = \frac{\log(N-1)}{N} + \frac{\gamma}{N} + \frac{\epsilon_{N-1}}{N}, \tag{30}$$

where γ is Euler's constant and $\epsilon_{N-1} \sim 1/2N$. Thus, we see that the mean interference is finite for all uniform distributions. For the particular case when $[a,b] = [0,2\pi]$, $\mathbb{E}(I) \to 1/\alpha$.

2) One-ring Correlation: Here, we have $\phi_i = 2\pi d \sin\theta_i$, where $\theta_i \sim U[0,2\pi]$. Hence,

$$\mathbb{E}[e^{jr\phi_i}] = \frac{1}{2\pi}\int_0^{2\pi} e^{jr2\pi d\sin(\theta_i)}d\theta_i = J_0(2\pi dr). \tag{31}$$

Substituting (31) into (27) we have $\mu_I^\infty = (1/\alpha)(1+2S)$, where

$$S = \lim_{N\to\infty}\left\{\sum_{r=1}^{N-1}\left(1-\frac{r}{N}\right)[J_0(2\pi dr)]^2\right\}. \tag{32}$$

From [31, eq. 10.17.3], for large arguments $J_0(z) = \sqrt{2/\pi z}\cos(z-\pi/4) + O(z^{-3/2})$. Hence, S exists (is finite) if and only if S_1 exists, where

$$\begin{aligned} S_1 &= \lim_{N\to\infty}\frac{1}{\pi^2 d}\sum_{r=1}^{N-1}\left(\frac{1}{r}-\frac{1}{N}\right)\cos^2\left(2\pi rd - \frac{\pi}{4}\right) \\ &\geq \lim_{N\to\infty}\frac{1}{\pi^2 d}\sum_{r=1}^{N-1}\frac{1}{r}\cos^2\left(2\pi rd-\frac{\pi}{4}\right) - \frac{1}{\pi^2 d}. \end{aligned} \tag{33}$$

Using the double angle formula, the first summation in (33) can be written as

$$\sum_{r=1}^{N-1}\frac{1}{r}\cos^2\left(2\pi rd-\frac{\pi}{4}\right) = \frac{1}{2}\sum_{r=1}^{N-1}\frac{1}{r} + \frac{1}{2}\sum_{r=1}^{N-1}\frac{1}{r}\sin(4\pi rd). \tag{34}$$

From [32, p. 43], the second sum in (34) is finite,

$$\frac{1}{2}\sum_{r=1}^{N-1}\frac{1}{r}\sin(4\pi rd) = \frac{\pi}{2} - 2\pi d \pmod{2\pi}, \tag{35}$$

and it is well-known that $(1/2)\sum_{r=1}^{N-1} 1/r$ diverges logarithmically. Thus, S_1 diverges, causing both S and μ_I^∞ to diverge. The simulation results in Section IV also support this claim.

D. Exponential Correlation Model Analysis in General

In Section III-B and Section III-C, we have analysed the asymptotic behaviour under extreme high correlation scenarios. We would also like to study the general behaviour of T_{ii}/T_{il}, which is the ratio of signal power $T_{ii} = \mathrm{tr}(\boldsymbol{\Sigma}_i^2)$ and interference power $T_{il} = \mathrm{tr}(\boldsymbol{\Sigma}_i\boldsymbol{\Sigma}_l)$. For simplicity, we only consider two users,

$$\frac{T_{ii}}{T_{il}} = \frac{\mathrm{tr}(\boldsymbol{\Sigma}_i^2)]}{\mathrm{tr}(\boldsymbol{\Sigma}_i\boldsymbol{\Sigma}_l)}. \tag{36}$$

For the exponential correlation model, we have

$$\begin{aligned} T_{ii} =& \sum_{i=1}^{N}(|\rho|^{2(i-1)} + |\rho|^{2(i-2)} + \cdots + 1 + |\rho|^2 + \cdots \\ & + |\rho|^{2(N-i)}) \\ =& \frac{N(1-|\rho|^4) - 2|\rho|^2(1-|\rho|^{2N})}{(1-|\rho|^2)^2}, \end{aligned} \tag{37}$$

and

$$\begin{aligned} T_{il} =& \sum_{i=1}^{N}(|\rho|^2 e^{j(\phi-\theta)(i-1)} + |\rho|^2 e^{j(\phi-\theta)(i-2)} + \cdots \\ & + 1 + |\rho|^2 e^{j(\theta-\phi)} + \cdots + |\rho|^2 e^{j(\theta-\phi)(N-i)}) \\ =& \frac{T_a + T_b + T_c}{T_d}, \end{aligned} \tag{38}$$

where

$$T_a = N(1-|\rho|^8) - 2N|\rho|^2\cos[(\theta-\phi)(1-|\rho|^4)], \tag{39}$$

$$T_b = -2|\rho|^2\cos(\theta-\phi) + 4|\rho|^4 - 2|\rho|^6\cos(\theta-\phi), \tag{40}$$

$$\begin{aligned} T_c =& 2|\rho|^{2N+2}\cos[(N+1)(\theta-\phi)] \\ & - 4|\rho|^{2N+4} + 2|\rho|^{2N+6}\cos[(N-1)(\theta-\phi)], \end{aligned} \tag{41}$$

$$T_d = \left[1 + |\rho|^4 - 2|\rho|^2\cos(\theta-\phi)\right]^2. \tag{42}$$

Substituting (37) and (38) into (36), we obtain the general expression of T_{ii}/T_{il}, which allows us to examine the correlation effect with various correlation coefficients.

E. Analog MRC Correlation Analysis

Next, we consider analog MRC and give new versions of the results in [25] which allow an interpretation of correlation effects. From [33, eq.15.3.3, p. 559], we have

$${}_2F_1(\alpha,\beta,\gamma;z) = (1-z)^{\gamma-\alpha-\beta}{}_2F_1(\gamma-\alpha,\gamma-\beta,\gamma;z).$$

Using this transformation formula allows the signal and interference power terms in (3) and [25] to be written as

$$\mathbb{E}\{|\hat{\mathbf{h}}_i^H\mathbf{h}_i|^2\} = N\beta_i + \frac{\pi}{4}\beta_i\sum_{\substack{j=1\\j\neq k}}^{N}\sum_{k=1}^{N}{}_2F_1\left(-\tfrac{1}{2},-\tfrac{1}{2},1;|\rho_{ijk}|^2\right), \tag{43}$$

$$\mathbb{E}\{|\hat{\mathbf{h}}_i^H\mathbf{h}_l|^2\} = N\beta_l + \frac{\pi\beta_l}{4}\sum_{\substack{j=1\\j\neq k}}^{N}\sum_{k=1}^{N}(\rho_{lkj}\rho_{ijk}){}_2F_1(\tfrac{1}{2},\tfrac{1}{2},2;|\rho_{ijk}|^2). \tag{44}$$

Using known results on hypergeometric functions, [33, eq.15.2.1, eq.15.1.1, and eq.15.1.20] we see that ${}_2F_1(-1/2,-1/2,1;|\rho_{ijk}|^2)$ and ${}_2F_1(1/2,1/2,2;|\rho_{ijk}|^2)$ both increase monotonically from 1 to $4/\pi$ as $|\rho_{ijk}|$ increases from 0 to 1, making (43)–(44) easier to interpret. We see that the mean signal power in (43) is an increasing function of $|\rho_{ijk}|$. The interference behaviour depends on the similarity of the correlation matrices. If $\boldsymbol{\Sigma}_i = \Sigma_l$, then $\rho_{lkj}\rho_{ijk} = |\rho_{ijk}|^2 > 0$ and interference grows with $|\rho_{ijk}|$. However, if $\boldsymbol{\Sigma}_i \neq \boldsymbol{\Sigma}_l$, then $\rho_{lkj}\rho_{ijk}$ is a complex constant and the sum in (44) will not necessarily grow with $|\rho_{ijk}|$ as terms may cancel. Again, we

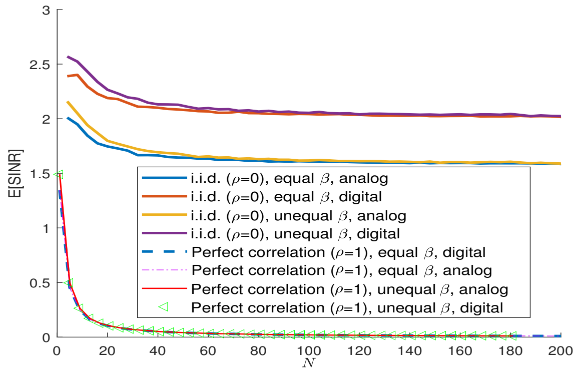

Fig. 1. $\mathbb{E}$[SINR] vs N for analog and digital MRC; i.i.d. and perfect correlation, equal and unequal link gains.

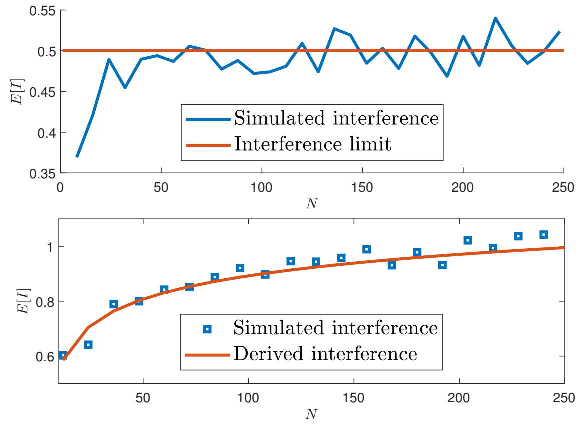

Fig. 2. $\mathbb{E}[I]$ vs N for perfectly correlated Rayleigh fading with unequal correlations (exponential-top, one-ring-bottom).

see the important property that correlation is detrimental with equal correlation but can be beneficial with sufficient variation across users.

IV. Numerical Results

The limiting results in Section III depend on the link gains, β_i. Thus, to examine convergence, we adopt a link gain model similar to that in [14], [34] where we consider scenarios of equal and unequal β_i values for each user. The equal link gain case serves as a reference with $\beta_i = 1$ for all users. The unequal case is modeled via a simple exponential decay for the β_i's as described in Section II. The decay is chosen so that the average link gain is $\bar{\beta} = 1$ and the desired user also has unit link gain. Fig. 1 shows the mean SINR vs N for analog and digital MRC with $P_{\rm t} = 1$ and $\alpha = 2$. We plot the mean rather than the instantaneous SINR to reduce variability and clearly identify the limits. Both the equal and unequal link gain scenarios are shown. The top four curves represent i.i.d. Rayleigh fading for which (14) and (20) give the limits 2 and $\pi/2$ which are verified in the figure. The unequal power case converges slightly more slowly as the power variation gives less averaging and stability compared to the equal power case. The bottom four curves correspond to perfect correlation with equal correlation matrices. As predicted by the analysis in (23), the mean SINR decays to zero.

Fig. 2 shows the mean interference of the exponential (top) and one-ring (bottom) models with perfect correlation and unequal correlation matrices. Equal link gains, $\alpha = 2$, and user specific angles, $\phi_i \sim U[0, 2\pi]$, are assumed. In the upper figure we see $\mathbb{E}[I]$ converging to the derived limit. In the lower figure, we see the interference (obtained by substituting (31) into (26)) agrees well with the simulated interference and grows logarithmically with N as predicted. Hence, the limiting behaviour is entirely different for the two models.

Next, we consider general levels of correlation between the benchmark results of i.i.d. and perfectly correlated channels. From (5) and (6), we see that $T_{ii} = \mathrm{tr}(\boldsymbol{\Sigma}_i^2)$ and $T_{il} = \mathrm{tr}(\boldsymbol{\Sigma}_i \boldsymbol{\Sigma}_l)$ control the effect of correlation on digital MRC. For the exponential correlation model, T_{ii} and T_{il} are given by (7) which is a function of ρ, N and $\Delta = \phi_i - \phi_l$. In Figs. 3 and 4 we plot T_{il} and T_{ii}/T_{il} against ρ and Δ for $N = 32$. The first measures interference while the second gives the size of the signal term relative to interference, a type of SIR. The interaction between the amplitude of the correlation parameter (ρ) and the difference in the phases of the correlation (Δ) is clear. Large amplitude correlation helps the signal relative to interference and reduces interference, thus enhancing SINR, unless the phases are very similar ($\Delta \approx 0$ or $\Delta \approx 2\pi$) when the SINR is adversely affected by large interference. Hence, as long as there is phase parameter diversity, increasing correlation is beneficial to performance. In Fig. 5 and Fig. 6 we plot the equivalent results for the one-ring model. We use (24) to compute $\boldsymbol{\Sigma}_i$ using $N = 32$ and note that correlation is controlled by the AS parameter where AS$= 0$ corresponds to perfect correlation and correlation drops as AS increases. User diversity is controlled by $\Delta_\theta = \phi_i - \phi_l$, the difference between the central angles of the two users. Figs. 5 and 6 are symmetric about $\Delta_\theta = \pi$ as the correlation matrices are the same for $\Delta_\theta = \Delta_1$ and $\Delta_\theta = \pi + \Delta_1$. Otherwise, the trends are identical to the exponential model where reducing angle spread (corresponding to increased correlation) is beneficial as long as there is diversity in the central angles of the users.

In Fig. 7 we show the simulated cumulative distribution function (CDF) of the mean SE for analog MRC assuming the exponential correlation structure. The randomness is due to the variation of drops including path loss and lognormal shadowing effects. The link gains are given by $\beta_i = A\zeta_i(d_0/d_i)^\gamma$, where d_i is the distance to the BS and ζ_i is lognormal shadowing. There are four users, each with a single antenna, uniformly located in a cell with the radius of 100 meters. The unit-less constant $A = 30$ dB, the reference distance $d_0 = 1$ meter, $N = 32$, the pathloss exponent $\gamma = 3.5$ and the standard deviation of shadowing is 6 dB. The transmit power $P_{\rm t}$ is chosen to guarantee that 95% of the time the SNR exceeds 0 dB. As predicted by the analysis, for a fixed correlation parameter (equal correlation matrices for the users) increasing the correlation decreases SE, whereas for differing correlation parameters (unequal correlation matrices for the

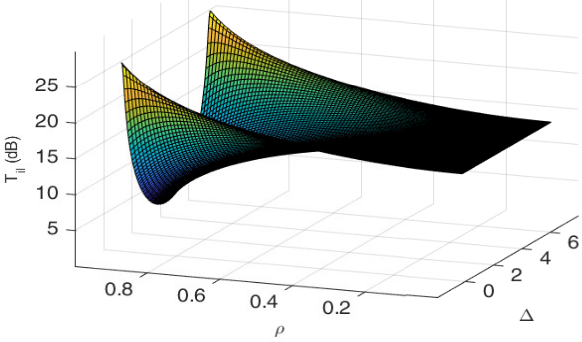

Fig. 3. T_{il} (dB) vs ρ and Δ; $N = 32$, exponential correlation.

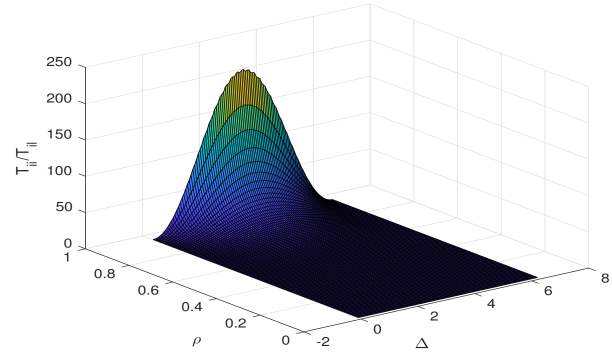

Fig. 4. T_{ii}/T_{il} vs ρ and Δ; $N = 32$, exponential correlation.

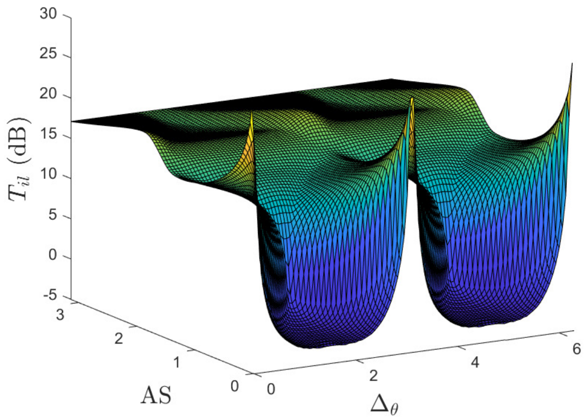

Fig. 5. T_{il} (dB) vs Δ and θ; $N = 32$, one-ring correlation.

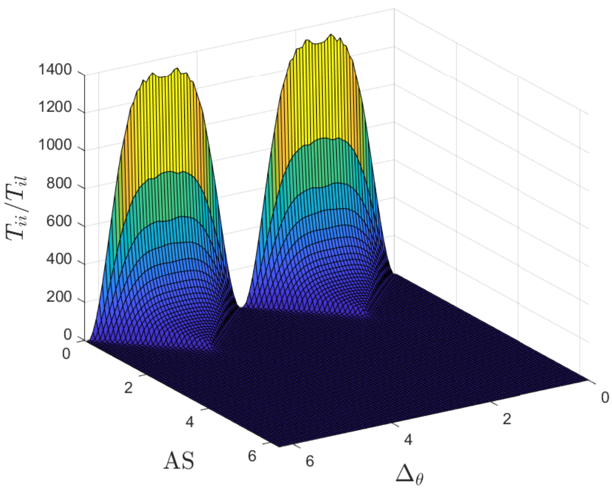

Fig. 6. T_{ii}/T_{il} vs Δ and θ; $N = 32$, one-ring correlation.

users), correlation improves the SE. The difference in SE can be very large so we next investigate how much of this variation is encountered with more realistic ray-based channels [3] based on clusters of scatterers. We adopt the measured angular parameters in [35]. The number of clusters $C = 3$, and the number of subpaths per cluster $L = 16$. Each subpath angle of arrival is modeled by a central cluster angle with a Gaussian distribution (zero mean and a standard deviation (σ_c) of $14.4°$) plus a subray offset angle which is Laplacian with a standard deviation (σ_l) of $6.24°$. Following [34], the cluster powers decay exponentially from cluster 1 to cluster C such that $C_c = (1/10)C_1$ and equal power among subrays is assumed. We also adopt another two sets of parameters, $C = 2, L = 20, \sigma_c = 2°, \sigma_l = 1°$ (narrow spread) and $C = 2, L = 20, \sigma_c = 30°, \sigma_l = 10°$ (wide spread), to compare with the parameters in [35]. From the figure, we can see that wider angular spreads increase system performance, which agrees with the results based on Rayleigh channels with unequal correlations. The SE based on measured parameters is similar to the Rayleigh results with less extreme values of ρ. Little change is observed as the angular spread is increased from $\sigma_c = 14.4°, \sigma_l = 6.24°$ to $\sigma_c = 30°, \sigma_l = 10°$ but considerable losses arise for the very narrow angle spread case ($\sigma_c = 2°, \sigma_l = 1°$). Hence, severe losses due to correlation are likely to be rare, but could exist, for example, in indoor non-line of sight environments where channels have limited numbers of clusters and narrow spread.

V. CONCLUSION

We have presented the first analysis of the effects of correlation on analog processing, compared analog to digital MRC and demonstrated that heterogeneous correlation effects extend to analog MRC. We have derived the expected signal and interference power, demonstrating that SIR decreases when the user correlation matrices are identical, but increases when they are different. We derived asymptotic SINR expressions for both analog and digital MRC for benchmark scenarios of uncorrelated and fully correlated Rayleigh channels, demonstrating that the performance is critically dependent on the correlation scenario. We have shown that for uncorrelated fading the SINR converges to a constant. For fully correlated channels

[3]Ray-based channel models assume that the signal arriving at an antenna is composed of multiple narrow beams (rays), originating from scattering clusters, see, e.g. [35].

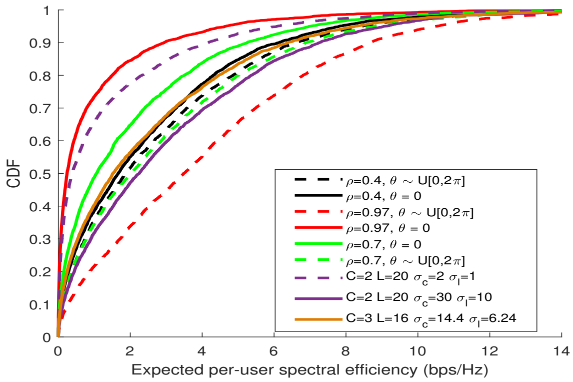

Fig. 7. Mean SE CDFs for Rayleigh and ray-based channels.

SINR converges to zero for equal correlation matrices, whereas for unequal correlation matrices SINR converges to zero or a constant, depending on the correlation model.

REFERENCES

[1] E. G. Larsson *et al.*, "Massive MIMO for next generation wireless systems," *IEEE Commun. Mag.*, vol. 52, no. 2, pp. 186–195, 2014.
[2] F. Rusek *et al.*, "Scaling up MIMO: Opportunities and challenges with very large arrays," *IEEE Signal Process. Mag.*, vol. 30, no. 1, pp. 40–60, 2013.
[3] P. J. Smith *et al.*, "SNAP POP for massive MIMO systems," in *Proc. IEEE ICC*, 2020.
[4] P. O. Akuon *et al.*, "Optimal error analysis of receive diversity schemes on arbitrarily correlated Rayleigh fading channels," *IET Commun.*, vol. 10, no. 7, pp. 854–861, 2016.
[5] S. Ikki *et al.*, "Performance analysis of cooperative diversity using equal gain combining (EGC) technique over Rayleigh fading channels," in *Proc. IEEE ICC*, 2007.
[6] R. K. Mallik *et al.*, "Performance of dual-diversity predetection EGC in correlated Rayleigh fading with unequal branch SNRs," *IEEE Trans. Commun*, vol. 50, no. 7, pp. 1041–1044, 2002.
[7] K. Sivanesan *et al.*, "The performance of the M-ary DS/CDMA cellular system over Rayleigh-fading channel with hybrid EGC-SC scheme," in *Proc. IEEE-VTS VTC*, 2000.
[8] S. Halunga *et al.*, "Error probability evaluation for RAKE reception of DS-CDMA signals with MRC and EGC combining in Rayleigh fading," in *Proc. IEEE TELSIKS*, 2007.
[9] R. K. Mallik *et al.*, "Performance of predetection dual diversity in correlated Rayleigh fading: EGC and SD," in *Proc. IEEE GLOBECOM*, 2000.
[10] A. Olutayo *et al.*, "Asymptotically tight performance bounds for equal-gain combining over a new correlated fading channel," in *Proc. IEEE CWIT*, 2017.
[11] Y. Song *et al.*, "Exact outage probability for equal gain combining with cochannel interference in Rayleigh fading," *IEEE Trans. Wireless Commun.*, vol. 2, no. 5, pp. 865–870, 2003.
[12] C. Masouros *et al.*, "Large-scale MIMO transmitters in fixed physical spaces: The effect of transmit correlation and mutual coupling," *IEEE Trans. Commun.*, vol. 61, no. 7, pp. 2794–2804, 2013.
[13] J. Hoydis *et al.*, "Massive MIMO in the UL/DL of cellular networks: How many antennas do we need?" *IEEE J. Sel. Areas Commun.*, vol. 31, no. 2, pp. 160–171, 2013.
[14] P. J. Smith *et al.*, "On the convergence of massive MIMO systems," in *Proc. IEEE ICC*, 2014.
[15] H. Tataria *et al.*, "General analysis of multiuser MIMO systems with regularized zero-forcing precoding under spatially correlated Rayleigh fading channels," in *Proc. IEEE ICC*, 2016.
[16] C. Zhang *et al.*, "Performance scaling law for multicell multiuser massive MIMO," *IEEE Trans. Veh. Technol.*, vol. 66, no. 11, pp. 9890–9903, 2017.
[17] A. Zanella *et al.*, "Performance of MIMO MRC in correlated Rayleigh fading environments," in *Proc. IEEE VTC*, 2005.
[18] R. H. Louie *et al.*, "Capacity approximations for multiuser MIMO-MRC with antenna correlation," in *Proc. IEEE ICC*, 2007.
[19] W. Belaoura *et al.*, "Effect of spatial correlation on the ergodic capacity for downlink massive MU-MIMO systems," in *Proc. IEEE ICSC*, 2017.
[20] H. Tataria *et al.*, "Spatial correlation variability in multiuser systems," in *Proc. IEEE ICC*, 2018.
[21] Ericsson, "Radio system portfolio for next generation access networks," 2019.
[22] F. Rusek, *et al.*, "Scaling up MIMO: Opportunities and challenges with very large arrays," *Signal Process. Mag. IEEE*, vol. 30, no. 1, pp. 40–60, 2012.
[23] J. Hoydis and others., "Massive mimo in the ul/dl of cellular networks: How many antennas do we need?" *IEEE J. Sel. Areas Commun.*, vol. 31, no. 2, pp. 160–171, 2013.
[24] P. J. Smith, C. T. Neil, M. Shafi, and P. A. Dmochowski, "On the convergence of massive mimo systems," 2014.
[25] S. Li *et al.*, "Analysis of analog and digital MRC for distributed and centralized MU-MIMO systems," *IEEE Trans. Veh. Technol.*, pp. 1948–1952, 2019.
[26] Q. Zhang, S. Jin, K.-K. Wong, H. Zhu, and M. Matthaiou, "Power scaling of uplink massive MIMO systems with arbitrary-rank channel means," *IEEE J. Sel. Topics Signal Process.*, vol. 8, no. 5, pp. 966–981, 2014.
[27] H. Tataria *et al.*, "Impact of line-of-sight and unequal spatial correlation on uplink MU-MIMO systems," *IEEE Wireless Commun. Lett.*, vol. 6, no. 5, pp. 634–637, 2017.
[28] B. Clerckx *et al.*, "Correlated fading in broadcast MIMO channels: Curse or blessing?" in *Proc. IEEE GLOBECOM*, 2008.
[29] A. M. Samoilenko, *Elements of the Mathematical Theory of Multi-frequency Oscillations*. Springer Science & Business Media, 2012.
[30] D.-S. Shiu *et al.*, "Fading correlation and its effect on the capacity of multielement antenna systems," *IEEE Trans. Commun.*, vol. 48, no. 3, pp. 502–513, 2000.
[31] F. W. Oliver, *NIST Handbook of Mathematical Functions*. Cambridge University Press, 2010.
[32] A. D. Wheelon, *Tables of Summable Series and Integrals Involving Bessel Functions*. Holden-Day, 1968.
[33] M. Abramowitz *et al.*, *Handbook of Mathematical Functions: with Formulas, Graphs, and Mathematical Tables*. Courier Corporation, 1964, vol. 55.
[34] S. Li *et al.*, "Massive MIMO for ray-based channels," in *Proc. IEEE ICC*, 2019.
[35] S. Sangodoyin *et al.*, "Cluster characterization of 3-D MIMO propagation channel in an urban macrocellular environment," *IEEE Trans. Wireless Commun.*, vol. 17, no. 8, pp. 5076–5091, 2018.

Shuang Li received a B.E. in Electronic Information Science and Technology in Underwater Acoustics from Harbin Engineering University, China, in 2007 and a Master's degree in Signal and Information Processing from Harbin Engineering University, China, in 2010. From 2010-2015, she worked with Huawei (Chengdu) as a system engineer and also in the public sector. She received a Ph.D. in Electronic Engineering from Victoria University of Wellington, New Zealand, in 2020. She is currently with Harbin Engineering University, China. Her research interests include system performance analysis in MU-MIMO wireless communication systems, intelligent communication systems, underwater acoustic communication and machine learning for future communication systems.

Peter J. Smith received the B.Sc degree in Mathematics and the Ph.D. degree in Statistics from the University of London, London, U.K., in 1983 and 1988, respectively. From 1983 to 1986 he was with the Telecommunications Laboratories at GEC Hirst Research Centre. From 1988 to 2001 he was a Lecturer in statistics at Victoria University of Wellington, New Zealand. From 2001-2015 he worked in Electrical and Computer Engineering at the University of Canterbury. In 2015 he joined Victoria University of Wellington as Professor of Statistics. He is also an Adjunct Professor in Electrical and Computer Engineering at the University of Canterbury, New Zealand and an Honorary Professor in the School of Electronics, Electrical Engineering and Computer Science, Queens University Belfast. He was elected a Fellow of the IEEE in 2015 and in 2017 was awarded a Distinguished Visiting Fellowship by the UK based Royal Academy of Engineering at Queens University Belfast. In 2018-2019 he was awarded Visiting Fellowships at the University of Bologna, the University of Bristol and the University of Melbourne. His research interests include the statistical aspects of design, modeling and analysis for communication systems, especially antenna arrays, MIMO, cognitive radio, massive MIMO and mmWave systems.

Pawel A. Dmochowski was born in Gdansk, Poland. He received a B.A.Sc (Engineering Physics) from the University of British Columbia, and M.Sc. and Ph.D. degrees from Queen’s University, Kingston, Ontario. He is currently with the School of Engineering and Computer Science at Victoria University of Wellington, New Zealand. Prior to joining Victoria University of Wellington, he was a Natural Sciences and Engineering Research Council (NSERC) Visiting Fellow at the Communications Research Centre Canada. In 2014-2015 he was a Visiting Professor at Carleton University in Ottawa. He is a Senior Member of the IEEE. Between 2014-2015 he was the Chair of the IEEE Vehicular Technology Society Chapters Committee. He has served as an Editor for IEEE Communications Letters and IEEE Wireless Communications Letters. His research interests include mmWave, massive MIMO and cognitive radio systems, with a particular emphasis on statistical performance characterisation.

Jingwei Yin received his B.S, M.S, and Ph.D. degrees in Underwater Acoustic Engineering from Harbin Engineering University, China in 1999, 2006, and 2007, respectively. He is a Visiting Professor at the Russian Far Eastern Federal University (FEFU). He is currently a Professor and Director of the Science and Technology Research Institute, Harbin Engineering University, China. He is the Deputy Director of the Underwater Acoustic branch of the Acoustical Society of China. He is also a Director of the Key Laboratory of Marine Information Acquisition and Security (Harbin Engineering University), Ministry of Industry and Information Technology. His research interests include underwater acoustic engineering, underwater acoustic communication, and polar acoustics.